Selectively Attenuating Soft Tissues Close to Sites of Inflammation in the Peritalar Region of Patients with Rheumatoid Arthritis Leads to Development of Pes Planovalgus

JAMES WOODBURN, MARK W. CORNWALL, ROGER W. SOAMES, PHILIP S. HELLIWELL

ABSTRACT. ***Objective.*** To compare the 3-dimensional (3D) orientation of the tibiotalar, tibiocalcaneal, and intertarsal joints in cadaveric specimens following structural weakening to predetermined ligaments in the peritalar region and medial ankle tendons under axial loads and simulated calcaneal valgus deformity.
Methods. Eight fresh-frozen, unembalmed human lower leg and foot specimens were placed in a materials testing machine. The mid-stance period of gait was simulated and the 3D orientation of the tibiotalar, tibiocalcaneal, and intertarsal joints was measured using an electromagnetic motion analysis system. Specimens were then axially loaded at 840 N for 5400 cycles with the calcaneus in its initial orientation and under simulated valgus conditions using a heel wedge following attenuation (multiple stab incisions) of selected ligaments (tibionavicular, anterior tibiotalar and tibiocalcaneal portions of the medial deltoid ligament, the inferior calcaneonavicular ligament, and the superomedial calcaneonavicular ligament) or tendons (tibialis posterior, flexor digitorum longus, and flexor hallucis longus). The joint orientation measurements were then repeated and compared with baseline intact measurements.
Results. Pes planovalgus was observed in 6/8 specimens following testing. The tibiotalar, tibiocalcaneal, talonavicular, and calcaneocuboid joints were more dorsiflexed, everted, and externally rotated following either ligament or tendon compromise. The changes in orientation were small but showed consistent patterns with the smallest changes (typically < 1°) for the transverse plane and largest (up to 3.5°) for the frontal plane. The magnitude of change was similar for the tibiotalar and tibiocalcaneal joints, largest for the talonavicular joint, and smallest for the calcaneocuboid joint for both ligament and tendon compromise. The orientation of the talocalcaneal joint was more plantarflexed and everted relative to baseline, for both the ligament and tendon compromise with < 1° of change in orientation about the transverse plane. Under simulated valgus heel conditions, joint orientation was further increased especially about the frontal plane in the direction of eversion. The smallest changes were noted for the calcaneocuboid joint (~ 1°), similar change (~ 2–3°) for the tibiotalar, tibiocalcaneal and talocalcaneal joints, and the largest changes (> 3°) for the talonavicular joint. There were no observed differences in the magnitude of change between ligament or tendon condition.
Conclusion. Selective attenuation to either the ligaments supporting the tibiotalar, talocalcaneal, and talonavicular joints or the medial ankle tendons followed by cyclic loading results in small but important changes in the orientation of the tarsal bones consistent with the development of pes planovalgus. (J Rheumatol 2005;32:268–74)

Key Indexing Terms:
RHEUMATOID ARTHRITIS   PES PLANOVALGUS   CADAVER MODEL

From the Academic Unit of Musculoskeletal Disease, University of Leeds, Leeds; Department of Physical Therapy, Northern Arizona University, Flagstaff, Arizona, USA; and School of Biomedical Sciences, University of Leeds, Leeds, UK.

Dr. Woodburn is a recipient of a Medical Research Council Clinician Scientist Fellowship.

J. Woodburn, BSc, PhD, SRCh; P.S. Helliwell, DM, PhD, FRCP, Academic Unit of Musculoskeletal Disease, University of Leeds; M.W. Cornwall, PhD, PT, CPed, Department of Physical Therapy, Northern Arizona University; R.W. Soames, BSc, PhD, School of Biomedical Sciences, University of Leeds.

Address reprint requests to Dr. J. Woodburn, Academic Unit of Musculoskeletal Disease, University of Leeds, 36 Clarendon Road, Leeds, LS2 9NZ, UK. E-mail: j.woodburn@leeds.ac.uk

Submitted April 7, 2004; revision accepted October 4, 2004.

In vitro models have been developed to study the pathophysiology and surgical treatment of pes planovalgus[1-5]. Physiological axial loads and tensile tendon loads are applied to specimens mounted in hydraulic testing machines[5] or custom foot-loading frames[1-6]. In these experiments, bone and/or joint alignment and standard radiographic angles are compared before and after soft tissue loading/unloading or following simulated injury comprising single or multiple transections of ligament and tendons[1-6]. These studies are relevant to understand normal structure and function and to quantify gross structural changes associated with dysfunction in the rearfoot and medial longitu-

dinal arch. However, techniques are also needed to model the underlying mechanical or disease processes associated with the early stages of pes planovalgus of the adult acquired-type. In inflammatory diseases, such as rheumatoid arthritis (RA), pes planovalgus rarely results from a single injury, but rather a gradual weakening of the structures as the result of continued and prolonged weight-bearing, with the ligamentous and tendonous structures becoming weakened because of persistent or repeated episodes of inflammation[7,8]. The clinical picture for pes planovalgus and the associated inflammatory and mechanical factors are well described in RA, but little is known about its evolution[7-11].

For *in vitro* models, stab incision may be a useful first approach to model partial tears in the medial ankle tendons associated with RA[8]. The findings of imaging studies that identified sites of joint inflammation in the tibiotalar, talocalcaneal, and intertarsal joints provide useful information to locate more precisely the ligaments to attenuate to model RA related pathology[7,8,10,12]. Altering the alignment of the rearfoot to match early deformity such as valgus heel can further refine the model, since the motion and associated orientation characteristics have been extensively described[10]. We compared the orientation of the tibiotalar, tibiocalcaneal, and intertarsal joints following (1) structural weakening of predetermined ligaments and tendons, and (2) simulated calcaneal valgus deformity.

MATERIALS AND METHODS

Anatomical specimens. Eight fresh-frozen unembalmed human lower leg and foot specimens were used in this study. Each limb was inspected for and excluded if significant rear- and/or mid-foot deformity, joint stiffness, ankylosis, or surface evidence of invasive surgery was present. The soft tissue (skin and muscle) of each anatomical specimen was removed from the proximal tibia and fibula to expose the flexor digitorum longus (FDL), flexor hallucis longus (FHL), and tibialis posterior (TP) tendons to approximately 80 mm proximal from the medial malleolus. The skin and subcutaneous fat were removed from the medial and dorsal ankle and foot to facilitate placement of motion sensors into the tibia and tarsal bones. The plantar aponeurosis, fat pad, and remaining soft tissue covering of the foot and ankle were left intact. Approximately 70 mm of exposed proximal tibia and fibula were embedded in polymethylmethacrylate encased within an aluminium vessel. Each specimen was mounted in a servohydraulic materials testing unit (Model 8500, Instron Corp., Canton, Massachusetts, USA). The specimen rested on a rigid plastic plate fixed to the actuator arm of the test machine with the lower leg visually aligned to vertical, with the foot perpendicular and neutral in both the transverse and frontal planes. Finally, a series of wire cables, clamps, and weights were used to secure and load the FHL, FDL, and TP tendons (Figure 1).

Instrumentation. Foot joint angles were recorded using a 3-dimensional electromagnetic motion analysis system (Skill Technologies Inc., Phoenix, AZ, USA) incorporating Fastrak motion tracking sensors (Polhemus, Colchester, VT, USA). The sensors measure 28 × 23 mm and have a mass of 17 g. A small hole was drilled in each bone and filled with polymethylmethacrylate cement into which a 4.7 mm plastic rod was inserted. Each rod protruded at an angle to avoid soft tissue impingement and to ensure adequate separation from neighboring sensors. Sensors were mounted on the rods by small plastic blocks.

During testing, the orientation of each sensor relative to the transmitter was captured by a microprocessor. Two systems were connected together,
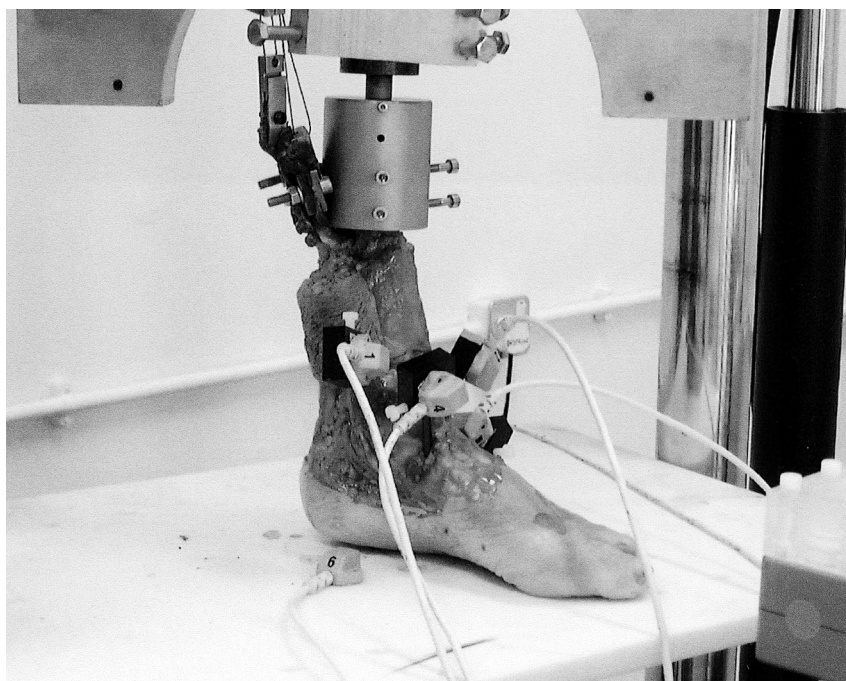

Figure 1. Experimental setup showing attachment of electromagnetic sensors to the cadaver specimen in the materials testing machine and the loading apparatus for the flexor hallucis longus, flexor digitorum longus, and tibialis posterior muscle tendons.

yielding a sampling rate for each sensor of 60 Hz. The resulting angles were smoothed using a 6 Hz low-pass digital Butterworth filter. A joint coordinate system was established for each joint studied according to the principles described by Grood and Suntay[13]. The joints investigated were the tibiocalcaneal, tibiotalar, talocalcaneal, talonavicular, and calcaneocuboid. Movement about a medial-lateral axis (X) was defined as dorsi(+)/plantarflexion(–), while motion about an anterior-posterior axis (Y) was termed inversion(+)/eversion(–). Finally, movement about a vertical axis (Z) through the proximal segment was defined as internal(+)/external(–) rotation.

Prior to testing, the data capture volume was mapped to create a correction algorithm to adjust the distortion of the electromagnetic field caused by metallic interference from the Instron machine. The correction algorithm was created using a commercial software package specifically designed for this purpose (SKMapper; Skill Technologies Inc., Phoenix, AZ, USA). The root mean square error following the mapping procedure was found to be < 1.0° for orientation for all axes of rotation.

Testing procedure. The zero reference orientation was established for all bones with the cadaveric foot resting on the plastic platform, the tibia perpendicular to the platform under a vertical compressive load of 240 N. Static baseline testing, designed to approximate the conditions typically found during the mid-stance phase of normal walking[14], consisted of a static axial compressive load of 560 N through a vertical tibia with the calcaneus assuming a resting orientation. This condition was termed the initial calcaneal orientation and does not assume that the calcaneus had either a neutral or vertical alignment. The orientation of each bone was recorded for a period of 10 s after the static load (560 N) had been applied for 20 s to precondition the soft tissues. During axial loading of the foot, the FDL, FHL, and TP tendons were loaded in tension based upon the unscaled values reported by Reeck, *et al* for the 30% stance period (24, 30, and 72 N, respectively)[15]. After this initial static baseline condition, either the TP tendon or the ligamentous and capsular support of the talonavicular, tibiotalar, and talocalcaneal joint of each specimen were compromised and joint orientations were measured under 2 conditions: A. initial calcaneal orientation (ICO) and B. simulated calcaneal valgus (SCV). An 8° valgus wedge was used to increase the deforming forces to enable the simulation of the valgus deformity typically found in RA[10]. Focal degeneration and partial tendon tears of TP, FDL, and FHL were modeled by using the ligament injury technique described by Niki, *et al*, which required multiple longitudinal incisions to be made parallel to the tendon fiber orientation, with care taken not to transect the structure[5]. Similarly, stab incisions were made through the tibionavicular, anterior tibiotalar and tibiocalcaneal portions of the medial deltoid ligament, the inferior calcaneonavicular ligament, and the superomedial calcaneonavicular ligament. At the talonavicular joint the incisions extended through the joint capsule into the joint space. Variable fiber orientation and blind access to the inferior calcaneonavicular ligament did not permit tight control of the direction and magnitude of the incisions. Figure 2 illustrates the order of testing used in this study.

Following ligament and/or tendon compromise, the specimens were subjected to axial compressive loading of 840 N with the foot in 8° of valgus for 5400 cycles at a frequency of 1 Hz. During cyclic loading, the TP, FHL, and FDL tendons continued to be loaded in tension. The purpose of the cyclic loading was to simulate repeated episodes of weight-bearing dur-
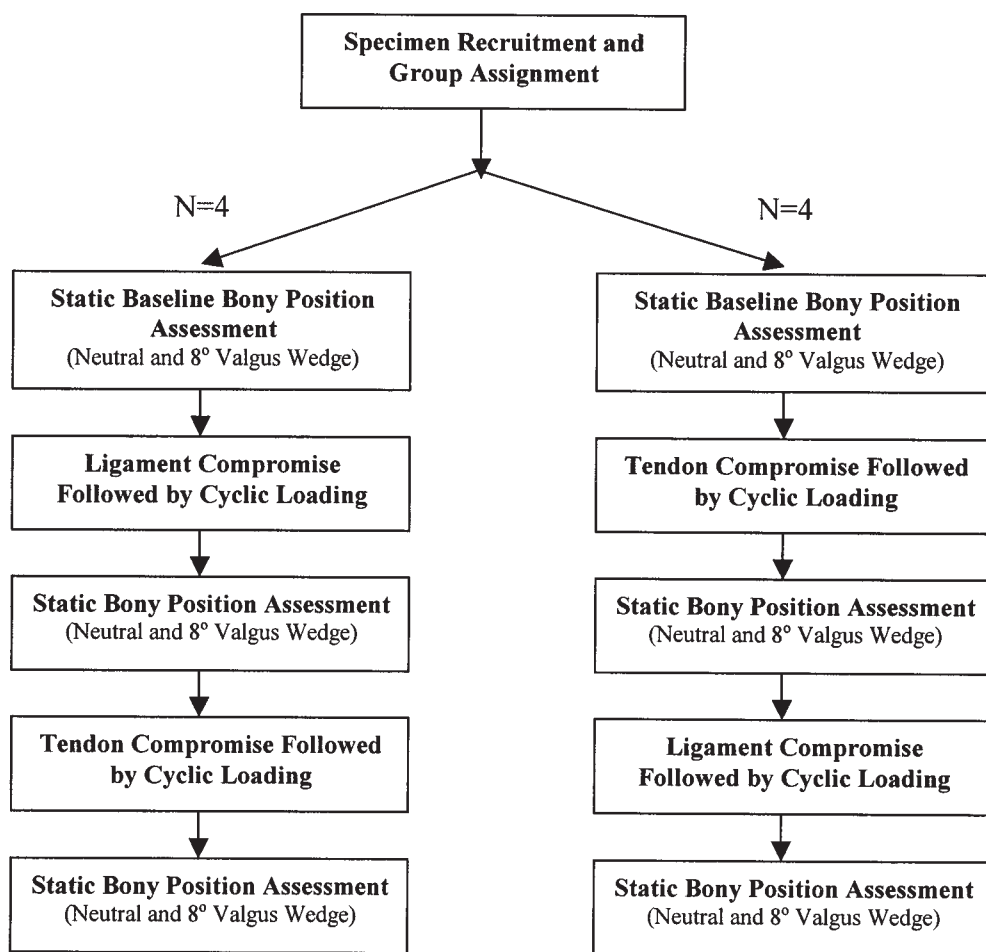

Figure 2. Summary of the experimental protocol.

ing walking. The number of cycles approximated the average daily steps taken by a typical community ambulatory person[4,5]. At the conclusion of the 5400 loading cycles, the angular orientation of each bone was again recorded using the protocol established under the initial static baseline condition of 560 N. The experiment proceeded according to the protocol outlined in Figure 2. The order of testing was reversed for pairs of specimens.

Data analysis. Means and standard deviations are given as descriptive statistics for the change in interosseous angles. Since the small sample size did not permit formal hypothesis testing, the t distribution was used to calculate mean differences and associated confidence intervals between the static baseline and the ligament and tendon compromise for both the ICO and the SCV conditions. The statistical software package SPSS for Windows version 9.0.0 was used.

RESULTS

Specimen observation during testing. From visual inspection and by the consensus of 2 observers during testing, changes in deformity consistent with the clinical description of pes planovalgus was observed in 6/8 specimens. This was characterized primarily by eversion (valgus) of the calcaneus and reduced medial longitudinal arch height, but less so by forefoot abduction. During cyclic loading, tears initially created by the stab incisions became visible and progressively increased in size in some ligaments, but no consistent pattern was observed across the specimens. Tendon rupture was not reported for any of the specimens.

Baseline joint angles. Changes in joint orientation were observed for all joints studied during static baseline testing; however, the magnitude of change varied by joint and plane of rotation (Table 1). The large standard deviations relative to the mean values indicated highly variable specimen response to the input loads. Across all joints a consistent pattern was observed, with the smallest changes for transverse (typically < 1°) and sagittal plane (< 2°) and larger changes (2° to 8°) for frontal plane orientation. In the frontal plane all joints were everted, with the largest changes noted for the talonavicular joint. Under SCV conditions the joints were resistant to further change in orientation compared to the ICO condition for all but the frontal plane. Here, all joints became more everted, with the largest change again noted for the talonavicular joint.

Ligament and tendon weakening. The joint orientations at baseline and post-ligament and tendon attenuation are shown in Table 1 and Figure 3. The tibiotalar, tibiocalcaneal, talonavicular, and calcaneocuboid joints were more dorsiflexed, everted, and externally rotated after either ligament or tendon compromise. The changes in orientation were small but showed consistent patterns, with the smallest changes (typically < 1°) for the transverse plane and largest (up to 3.5°) for the frontal plane. The magnitude of change was similar for the tibiotalar and tibiocalcaneal joints, largest for the talonavicular joint, and smallest for the calca-

Table 1. Joint orientation (degrees) at baseline and under initial calcaneal orientation and simulated calcaneal valgus conditions, including mean difference (95% CI of the difference) between conditions.

Joint	Condition	Joint Motion Parameter	Angle at Baseline (A) Mean (SD)	Angle after Ligament (B) Mean (SD)	Diff B-A (Mean, 95% CI)	Angle after Tendon (C) Mean (SD)	Diff C-A (Mean, 95% CI)
Tib-Tal	ICO	D/P Flex	1.1 (0.6)	2.6 (2.8)	1.5 (-0.8,3.7)	3.3 (2.8)	2.2 (-.5,4.4)
		Inv/Ever	-2.4 (1.9)	-4.9 (4.3)	-2.5 (-4.9,0)	-4.9 (4.6)	-2.5 (-5.2,0.2)
		I/R Rot	0.0 (1.5)	-0.6 (2.6)	-0.6 (-2.3, 1.1)	0.1 (2.5)	.1 (-1.5,1.7)
	SCV	D/P Flex	0.8 (0.8)	2.6 (2.6)	1.8 (-0.2, 3.7)	2.1 (1.3)	1.3 (.5,2.2)
		Inv/Ever	-3.8 (2.1)	-6.8 (4.4)	-2.9 (-5.7,-0.2)	-6.2 (4.4)	-2.4 (-5.0, 0.3)
		I/R Rot	0.5 (2.0)	-0.1 (2.9)	-0.6 (-2.2,1.1)	-0.5 (2.7)	0.0 (-1.5,1.5)
Tib-Calc	ICO	D/P Flex	1.1 (0.6)	3.0 (2.3)	1.9 (0,3.7)	3.3 (2.8)	2.2 (0,4.4)
		Inv/Ever	-2.4 (1.9)	-4.9 (4.3)	-2.6 (-5.1,0)	-4.9 (4.6)	-2.5 (-5.2,0.2)
		I/R Rot	0.2 (1.5)	-0.8 (2.1)	-1.0 (-2.0,0.1)	-1.2 (2.2)	-1.3 (-2.4,-0.3)
	SCV	D/P Flex	0.8 (0.8)	2.6 (2.6)	1.8 (-0.2,3.7)	2.1 (1.3)	1.3 (0.5,2.2)
		Inv/Ever	-3.8 (2.1)	-6.8 (4.4)	-2.9 (-5.7,-0.2)	-6.2 (4.4)	-2.4 (-5.0,0.25)
		I/R Rot	0.1 (2.0)	-0.8 (2.7)	-0.8 (-2.4,0.7)	-0.3 (2.7)	-0.4 (-1.8,1.0)
Tal-Calc	ICO	D/P Flex	-1.1 (1.6)	-1.4 (2.3)	-0.4 (-1.4,0.6)	-1.6 (2.4)	-0.5 (-1.7,0.7)
		Inv/Ever	-2.9 (2.3)	-5.1 (4.8)	-2.4 (-5.1,0.3)	-5.2 (4.9)	-2.3 (-5.0,0.4)
		I/R Rot	-0.5 (2.8)	0.2 (5.4)	0.4 (-4.1,4.9)	-0.7 (5.3)	-0.2 (-4.0,3.5)
	SCV	D/P Flex	-1.6 (1.7)	-2.1 (2.4)	-0.5 (-1.5 0.5)	-2.1 (2.7)	-0.5 (-1.8,0.9)
		Inv/Ever	-4.1 (2.9)	-6.6 (4.9)	-2.5 (-5.4,0.3)	-6.2 (4.7)	-2.1 (-4.7,0.5)
		I/R Rot	-0.4 (3.7)	0.3 (6.4)	0.7 (-4.0,5.4)	-0.7 (5.4)	-0.4 (-3.5,2.6)
Talo-Nav	ICO	D/P Flex	-1.7 (2.1)	-2.1 (3.6)	-0.7 (-2.3,1.0)	-2.0 (3.2)	-0.4 (-1.8,1.1)
		Inv/Ever	-5.8 (3.6)	-8.9 (6.4)	-3.4 (-6.6,-0.2)	-9.2 (7.1)	-3.4 (-7.1,0.2)
		I/R Rot	-0.9 (5.5)	-1.0 (10.0)	-1.0 (-7.3,5.4)	-2.3 (9.8)	-1.5 (-6.5,3.5)
	SCV	D/P Flex	-1.6 (2.2)	-2.1 (3.5)	-0.5 (-1.9,1.0)	-2.1 (3.0)	-0.4 (-1.5,0.7)
		Inv/Ever	-7.9 (4.7)	-11.7 (7.2)	-3.7 (-7.2,-0.3)	-11.4 (7.4)	-3.4 (-7.0,0.2)
		I/R Rot	-1.2 (6.4)	-1.4 (10.9)	-0.2 (-6.1,5.8)	-2.8 (9.6)	-1.6 (-5.7,2.6)
Calc-Cub	ICO	D/P Flex	-0.6 (1.2)	-0.7 (1.5)	-0.1 (-0.6,0.4)	-0.7 (0.6)	-0.1 (-0.6,0.4)
		Inv/Ever	-2.3 (1.2)	-2.8 (1.5)	-0.8 (-2.0,0.4)	-2.9 (1.7)	-0.6 (-1.5,0.3)
		I/R Rot	-0.2 (2.6)	-1.0 (3.7)	-1.2 (-2.9,0.4)	-1.2 (3.7)	-1.1 (-2.2,0.1)
	SCV	D/P Flex	-0.3 (0.5)	-0.5 (0.8)	-0.1 (-0.7,0.4)	-0.5 (0.8)	-0.1 (-0.7,0.4)
		Inv/Ever	-3.5 (1.8)	-4.5 (2.1)	-1.0 (-1.5,-0.5)	-4.6 (2.2)	-1.1 (-1.7,-0.5)
		I/R Rot	-0.3 (3.2)	-1.0 (4.2)	-0.7 (-1.6,0.3)	-1.2 (4.2)	-0.9 (-1.9,0.1)

Diff: difference; ICO: initial calcaneal orientation; SCV: simulated calcaneal valgus; Tib-Tal: tibiotalar joint; Tib-Calc: tibiocalcaneal joint; Tal-Calc: talocalcaneal joint; Talo-Nav: talonavicular joint; Calc-Cub: calcaneocuboid joint; D/P Flex: dorsiflexion (+)/plantarflexion (–) in sagittal plane; Inv/Ever: inversion (+)/eversion (–) in frontal plane; I/R Rot: internal (+)/external (–) rotation in transverse plane.
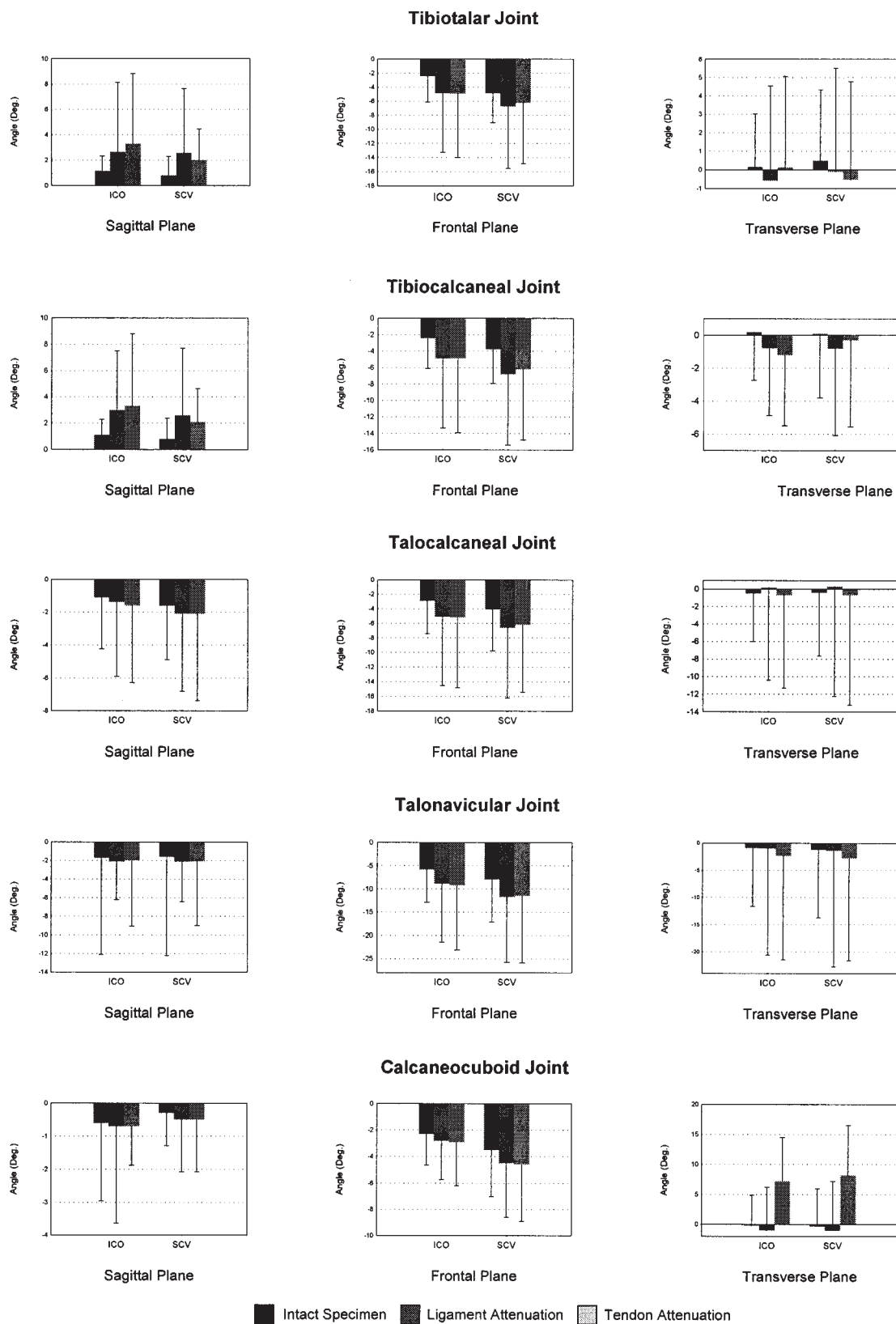
Tibiotalar Joint

Sagittal Plane | Frontal Plane | Transverse Plane

Tibiocalcaneal Joint

Sagittal Plane | Frontal Plane | Transverse Plane

Talocalcaneal Joint

Sagittal Plane | Frontal Plane | Transverse Plane

Talonavicular Joint

Sagittal Plane | Frontal Plane | Transverse Plane

Calcaneocuboid Joint

Sagittal Plane | Frontal Plane | Transverse Plane

■ Intact Specimen   ▨ Ligament Attenuation   ▨ Tendon Attenuation

Figure 3. Joint orientation (degrees) at baseline and post-ligament and tendon attenuation under initial calcaneal orientation (ICO) and simulated calcaneal valgus (SCV) conditions.

neocuboid joint for both ligament and tendon compromise. The orientation of the talocalcaneal joint was more plantarflexed and everted relative to the baseline, for both the ligament and tendon compromise, with < 1° of change in orientation about the transverse plane. The wide 95% confidence intervals for the mean difference indicate large variation in the response of specimens to simulated ligament and tendon damage.

Simulated calcaneal valgus. Under SCV conditions, for both the ligament and tendon compromise the orientation of all joints was further changed (Table 1 and Figure 3). Where changes of > 1° were observed, the magnitude of the orientation was increased and always in the same direction of the initial change from baseline to ICO condition. Again, the largest change in orientation was in the frontal plane in the direction of eversion, with the smallest change noted for the calcaneocuboid joint (~ 1°), similar change (~ 2°–3°) for the tibiotalar, tibiocalcaneal and talocalcaneal joints, and the largest changes (> 3°) for the talonavicular joint. There were no observed differences in the magnitude of change between ligament or tendon condition. From the static baseline tests, the orientation of the talonavicular joint changed by ~ 11° for both the ligament and tendon compromise.

DISCUSSION

The medial ankle and tarsal joint ligaments have important motion guiding and stabilizing functions[2,15,16], and tibialis posterior is considered the major muscle maintaining the medial longitudinal arch[1,17]. Disease processes that weaken these tissues structurally, such as inflammatory arthritis, may lead to collapse of the medial longitudinal arch and valgus of the hindfoot[1,2,6]. Our results show that selectively attenuating such structure by minimally invasive injury led to changes in the orientation of the tarsal bones, and deformity consistent with the clinical description of pes planovalgus.

Under normal physiological loads the largest tarsal joint rotations are found at the talonavicular joint, especially for frontal plane motion[18,19]. This joint remains stable because the inferior calcaneonavicular ligament and the superomedial calcaneonavicular ligament are force-bearing and resist medial and plantar displacement of the talar head, assisted by the expansive insertion and blending of tibialis posterior to the tuberosity of the navicular[5,15]. This joint is vulnerable to synovitis in RA[11], so it was appropriate to selectively attenuate these structures, and doing so resulted in the largest observed changes in joint orientation in the direction of increased eversion. Moreover, equivalent changes were noted independent of the sequence of testing, confirming the structural interdependency of the ligaments and tendon. The superomedial portion of the calcaneonavicular ligament assumes the greater biomechanical role, but these structures are functionally interrelated, since calcaneonavicular ligament insufficiency is frequently encountered with tibialis

posterior tendon dysfunction[20]. This association is important, as the method of attenuating these structures through stab incisions was unlikely to truly isolate ligament and tendon pathology in this region. Further, when tibialis posterior is dysfunctional, the midfoot loses its rigidity and stability during the latter part of stance[20,21]. The powerful gastro-soleus complex then acts across the talonavicular joint as well as the forefoot during propulsion, and the resultant motion is thought to stretch the calcaneonavicular and medial plantar ligaments[20,21]. It should be remembered that the observed changes in orientation were created with the foot in a mid-stance posture under axial load, and that further changes may have been expected had we been able to simulate foot orientation during propulsion with the gastro-soleus complex simultaneously under tension.

Although tibialis posterior tendon rupture is uncommon — a series of 3 imaging studies found the prevalence to be < 5% among RA cases with pes planovalgus — the tendon may attenuate within its structure and thus become dysfunctional[8,21-23]. Our study confirmed this view, and the changes in bone orientation were small but consistent with those reported earlier[5]. Nevertheless, while the model was intended to be specifically relevant to RA, the resulting pes planovalgus may have been no different from other adult progressive flatfoot deformity of any etiology, such as trauma or tibialis posterior tendon rupture. Paradoxically, dysfunction has been characterized by muscle weakness in the presence of increased electromyographic activity, and its role in the pathogenesis of pes planovalgus in RA remains unclear[8,12,21,22,24]. The relevant functional input for all stages of disease with appropriately scaled tensions to simulate normal and weak muscle groups, and the action of antagonists, primarily the peroneal muscle groups, will be included in future models.

Although the primary site for ligament attenuation was the medial aspect of the foot, changes in joint orientation were expected for all the tarsal joints, since their movement patterns are coupled[19]. Our findings were consistent with other studies simulating both ligament and tendon compromise[1-6]. The absolute changes were small, but consistent with reports where experimental protocols included complete sectioning of structures[2]. For example, Kitaoka, *et al* defined the relative contribution of 6 ligaments in stabilizing the arch and found changes in orientation of the tarsal bones of typically less than 2°[2]. This emphasizes the importance of the mode of injury, where, in this study, cyclic loading may have caused significant stretching of soft tissue.

The tibionavicular, anterior tibiotalar, and tibiocalcaneal portions of the medial deltoid ligament were attenuated on the basis that the tibiotalar joint is involved in RA[11]. We observed changes in eversion orientation and small amounts of internal tibial rotation through the tibiotalar and the tarsal joints, with eversion increasing further when specimens were wedged into a valgus position. The effect was subject

to considerable variability among specimens, but these changes are consistent with the findings of other studies[9,10]. Importantly, the dominant frontal plane changes resulted in a valgus heel deformity typical of that seen in patients with RA[9,10]. Recently, attention has been paid to degeneration of the interosseous talocalcaneal and cervical ligaments associated with inflammation in the sinus tarsi region[8,12]. We speculate that attenuating these ligaments may subject specimens to further deformity, because they are important stabilizers of the talocalcaneal joint[25]. Interestingly, we observed that soft tissue compromise medially resulted in small changes in joint orientation at the calcaneocuboid joint, thus confirming the complex properties of foot motion and the potential for widespread changes in function following injury.

In summary, compromise to either the ligaments supporting the tibiotalar, talocalcaneal, and talonavicular joints or the medial ankle tendons results in small but important changes in the orientation of the tarsal bones consistent with the development of pes planovalgus. We intend to use this experimental method to study and develop mechanical interventions directed at stabilizing the foot, primarily through functional foot orthoses.

REFERENCES

1. Kitaoka HB, Luo ZP, An KN. Effect of the posterior tibial tendon on the arch of the foot during simulated weightbearing: biomechanical analysis. Foot Ankle Int 1997;18:43-6.
2. Kitaoka HB, Ahn T-K, Luo ZP, An KN. Stability of the arch of the foot. Foot Ankle Int 1997;18:644-8.
3. Kitaoka HB, Luo ZP, An KN. Three-dimensional analysis of flatfoot deformity: cadaver study. Foot Ankle Int 1998;19:447-51.
4. McCormack AP, Niki H, Kiser P, Tencer AF, Sangeorzan BJ. Two reconstructive techniques for flatfoot deformity comparing contact characteristics of the hindfoot joints. Foot Ankle Int 1998;19:452-61.
5. Niki H, Ching RP, Kiser P, Sangeorzan BJ. The effect of posterior tibial tendon dysfunction on hindfoot kinematics. Foot Ankle Int 2001;22:292-300.
6. Imhauser CW, Siegler S, Abidi NA, Frankel DZ. The effect of posterior tibialis tendon dysfunction on the plantar pressure characteristics and the kinematics of the arch and the hindfoot. Clin Biomech 2004;19:161-9.
7. Woodburn J, Udupa JK, Hirsch BE, et al. The geometrical architecture of the subtalar and midtarsal joints in rheumatoid arthritis based on MR imaging. Arthritis Rheum 2002;46:3168-77.
8. Jernberg ET, Simkin P, Kravette M, Lowe P, Gardner G. The posterior tibial tendon and tarsal sinus in rheumatoid flat foot: magnetic resonance imaging of 40 feet. J Rheumatol 1999;26:289-93.
9. Turner DE, Woodburn J, Helliwell PS, Cornwall ME, Emery P. Pes planovalgus in rheumatoid arthritis: a descriptive and analytical study of foot function determined by gait analysis. Musculoskeletal Care 2003;1:21-33.
10. Woodburn J, Helliwell PS, Barker S. Three-dimensional kinematics at the ankle joint complex in rheumatoid arthritis patients with painful valgus deformity of the rearfoot. Rheumatology Oxford 2002;41:1406-12.
11. Lehtinen A, Paimela L, Kreula J, Leirisalo-Repo M, Taavitsainen M. Painful ankle region in rheumatoid arthritis. Acta Radiol 1996;37:572-7.
12. Bouysset M, Tebib J, Tavernier T, et al. Posterior tibial tendon and subtalar joint complex in rheumatoid arthritis: magnetic resonance imaging study. J Rheumatol 2003;30:1951-4.
13. Grood ES, Suntay WJ. A joint coordinate system for the clinical description of three-dimensional motions: application to the knee. J Biomech Eng 1983;105:136-44.
14. Chao E, Laughman RK, Schneider E, Stauffer RN. Normative data of knee joint motion and ground reaction forces in adult level walking. J Biomech 1983;16:219-33.
15. Reeck J, Felten N, McCormack AP, Kiser P, Tencer AF, Sangeorzan BJ. Support of the talus: a biomechanical investigation of the contributions of the talonavicular and talocalcaneal joints, and the superomedial calcaneonavicular ligament. Foot Ankle Int 1998;19:674-82.
16. Leardini A, O'Connor JJ, Catani F, Giannini S. A geometric model of the human ankle joint. J Biomech 1999;32:585-91.
17. Klein P, Mattys S, Rooze M. Moment arm length variations of selected muscles acting on the talocrural and subtalar joints during movement: an in vitro study. J Biomech 1996;29:21-30.
18. Kitaoka HB, Lundberg A, Luo ZP, An KN. Kinematics of the normal arch of the foot and ankle under physiological loading. Foot Ankle Int 1995;16:492-9.
19. Lundberg A, Svensson OK, Bylund C, Goldie I, Selvik G. Kinematics of the ankle/foot complex — part 2: pronation and supination. Foot Ankle Int 1989;9:248-53.
20. Yao L, Gentili A, Cracchiolo A. MR imaging findings in spring ligament insufficiency. Skeletal Radiol 1999;28:245-50.
21. Coakley FV, Smanta AK, Finlay DB. Ultrasonography of the tibialis posterior tendon in rheumatoid arthritis. Br J Rheumatol 1994;33:273-7.
22. Masterton E, Mulcahy D, McElwain J, McInerney D. The planovalgus rheumatoid foot: is tibialis posterior rupture a factor. Br J Rheumatol 1995;34:645-6.
23. Premkumar A, Perry, MB, Dwyer AJ, et al. Sonography and MR imaging of posterior tibial tendinopathy. AJR Am J Roentgenol 2002;178:223-32.
24. Keenan MAE, Peabody TD, Gronley JK, Perry J. Valgus deformity of the feet and characteristics of gait in patients who have rheumatoid arthritis. J Bone Jt Surg Am 1991;73:237-47.
25. Kjaersgaard-Andersen P, Wethelund JO, Helmig P, Soballe K. The stabilising effect of the ligamentous structures in the sinus and canalis tarsi on movements in the hindfoot. Am J Sports Med 1988;16:512-6.